ELSEVIER

Biochimica et Biophysica Acta 1459 (2000) 191–201

BIOCHIMICA ET BIOPHYSICA ACTA

BBA

www.elsevier.com/locate/bba

# Conformational relaxation following reduction of the photoactive bacteriopheophytin in reaction centers from *Blastochloris viridis*. Influence of mutations at position M208

F. Müh [a], M. Bibikova [b], E. Schlodder [a], D. Oesterhelt [b], W. Lubitz [a,*]

[a] *Max-Volmer-Institut für Biophysikalische Chemie und Biochemie, Technische Universität Berlin, Strasse des 17. Juni 135, D-10623 Berlin, Germany*

[b] *Max-Planck-Institut für Biochemie, Am Klopferspitz 18a, D-82152 Martinsried, Germany*

Received 7 February 2000; received in revised form 11 May 2000; accepted 17 May 2000

**Abstract**

The photochemically trapped bacteriopheophytin (BPh) *b* radical anion in the active branch ($\Phi_A^{\bullet-}$) of reaction centers (RCs) from *Blastochloris* (formerly called *Rhodopseudomonas*) *viridis* is characterized by $^1$H-ENDOR as well as optical absorption spectroscopy. The two site-directed mutants YF(M208) and YL(M208), in which tyrosine at position M208 is replaced by phenylalanine and leucine, respectively, are investigated and compared with the wild type. The residue at M208 is in close proximity to the primary electron donor, P, the monomeric bacteriochlorophyll (BChl), $B_A$, and the BPh, $\Phi_A$, that are involved in the transmembrane electron transfer to the quinone, $Q_A$, in the RC. The analysis of the ENDOR spectra of $\Phi_A^{\bullet-}$ at 160 K indicates that two distinct states of $\Phi_A^{\bullet-}$ are present in the wild type and the mutant YF(M208). Based on a comparison with $\Phi_A^{\bullet-}$ in RCs of *Rhodobacter sphaeroides* the two states are interpreted as torsional isomers of the 3-acetyl group of $\Phi_A$. Only one $\Phi_A^{\bullet-}$ state occurs in the mutant YL(M208). This effect of the leucine residue at position M208 is explained by steric hindrance that locks the acetyl group in one specific position. On the basis of these results, an interpretation of the optical absorption difference spectrum of the state $\Phi_A^{\bullet-}Q_A^{\bullet-}$ is attempted. This state can be accumulated at 100 K and undergoes an irreversible change between 100 and 200 K [Tiede et al., Biochim. Biophys. Acta 892 (1987) 294–302]. The corresponding absorbance changes in the BChl $Q_x$ and $Q_y$ regions observed in the wild type also occur in the YF(M208) mutant but *not* in YL(M208). The observed changes in the wild type and YF(M208) are assigned to RCs in which the 3-acetyl group of $\Phi_A$ changes its orientation. It is concluded that this distinct structural relaxation of $\Phi_A$ can significantly affect the optical properties of $B_A$ and contribute to the light-induced absorption difference spectra. 

*Keywords:* Acetyl group reorientation; Bacteriopheophytin; Electron nuclear double resonance; Optical difference spectrum; Photosynthetic charge separation; Purple bacterium; *Blastochloris viridis*

Abbreviations: $\theta$, dihedral angle of the acetyl group (see Fig. 2); $\Phi_{A,B}$, BPh in the A- and B-branch, respectively (also referred to in the literature as $H_{A,B}$ or $H_{L,M}$); $A$, hfc constant; $A_{iso}$, isotropic hfc constant; $A_\perp$, $A_\parallel$, perpendicular and parallel components of uniaxial hfc tensors; BChl, bacteriochlorophyll; BPh, bacteriopheophytin; ENDOR, electron nuclear double resonance; EPR, electron paramagnetic resonance; ET, electron transfer; hfc, hyperfine coupling; P, primary donor; $Q_A$, primary quinone; $Q_B$, secondary quinone; $Q_{x,y}$, optical transitions in BChls and BPhs; RC, reaction center; rf, radiofrequency; TRIPLE, electron nuclear nuclear triple resonance

* Corresponding author. Fax: +49-30-314-21122; E-mail: lubitz@echo.chem.tu-berlin.de

0005-2728/00/$ – see front matter 
PII: S0005-2728(00)00147-X

## 1. Introduction

The key step of bacterial photosynthesis is the light-induced charge separation across the intracytoplasmic membrane that occurs in the so-called reaction center (RC). The RC is a membrane-spanning pigment–protein complex that contains two symmetry-related branches of cofactors (Fig. 1), held in place by the L- and M-protein subunits. These cofactors are a dimer of bacteriochlorophyll (BChl) molecules ($P_L$ and $P_M$; the primary donor P), two monomeric BChls ($B_A$ and $B_B$), two monomeric bacteriopheophytins (BPhs; $\Phi_A$ and $\Phi_B$), two quinones ($Q_A$ and $Q_B$), one carotenoid molecule and one non-heme iron [1,2]. Despite their $C_2$-symmetric arrangement only the cofactors in the A-branch, namely $B_A$, $\Phi_A$ and $Q_A$, act as intermediate electron acceptors for the electron flow from the lowest excited singlet state of P to the final acceptor $Q_B$ [3]. The first intermediate state, $P^{\bullet+}B_A^{\bullet-}$, is formed in $\sim$3 ps after excitation of P. $B_A^{\bullet-}$ is short-lived and reduces the subsequent acceptor $\Phi_A$ in less than 1 ps. The further reaction to $P^{\bullet+}Q_A^{\bullet-}$ takes place within $\sim$200 ps. During this time period – or on longer timescales, when electron transfer (ET) to $Q_A$ is blocked – the state $P^{\bullet+}\Phi_A^{\bullet-}$ is believed to undergo structural relaxation processes that are manifested in complex kinetics of absorbance differences [4,5] and delayed fluorescence from P* [6,7].

In a similar way, the radical anion $\Phi_A^{\bullet-}$, which can be freeze-trapped in bacterial RCs in the presence of an exogenous electron donor [8–10], may relax after its formation in order to minimize the free energy of the system. This radical anion must be stabilized for the investigation of its electronic structure with ENDOR or TRIPLE resonance spectroscopy [10,11]. Using these techniques it could recently be demonstrated that the BPh *a* radical anion in isolated RCs from *Rhodobacter sphaeroides* can be trapped in a metastable form, termed $I_1^{\bullet-}$, which relaxes at temperatures above 150 K to a second distinct conformation, called $I_2^{\bullet-}$ [12,13].

Tyrosine (Tyr) M208 in RCs from *Blastochloris* (formerly called *Rhodopseudomonas* [14]) *viridis* and *Rhodobacter capsulatus*, which is homologous to M210 in *R. sphaeroides*, is considered to be an important amino acid residue in bacterial RCs, since it is highly conserved and in close proximity to the photochemically active cofactors P, $B_A$, and $\Phi_A$ (Fig. 1). Site-specific mutagenesis at this position in *R. capsulatus* [15], *R. sphaeroides* [16], and *B. viridis* [17] has been used extensively to elucidate a possible functional role of this residue in the ET process. Replacement of Tyr M208/M210 with either Phe, Leu, Ile, Trp, Thr or Glu causes a dramatic retardation of the primary charge separation [15,17–21], whereas replacement with His causes only marginal changes [15,22]. The influence of Tyr M208/M210 on the ET rate was mainly explained by an electrostatic effect on the energy level of the state $P^{\bullet+}B_A^{\bullet-}$ [20,23,24]. Recently, it was shown that the charge separation involves $P^{\bullet+}B_A^{\bullet-}$ as a real intermediate also in the mutants YF(M210) and YL(M210), where this state is assumed to be energetically raised [25]. It should be noted that in these mutations direct excitation of $B_A$ can also lead to the formation of $P^{\bullet+}Q_A^{\bullet-}$ via alternative pathways [26–29]. These results corroborate the view that the state $P^{\bullet+}B_A^{\bullet-}$ is a real intermediate in the charge separation processes.

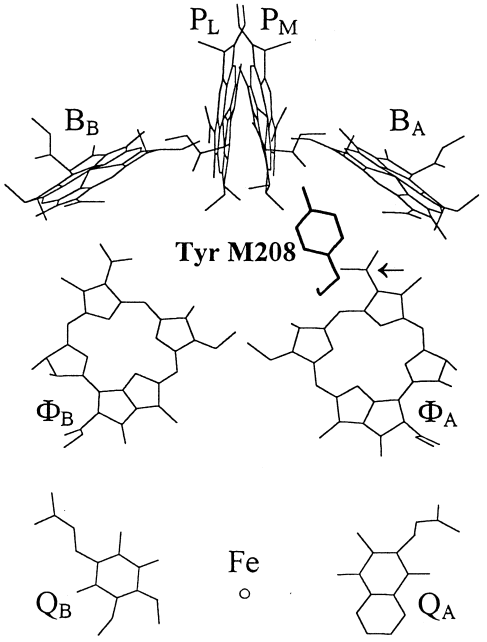


Fig. 1. X-ray crystallographic structure [1] of the cofactors $P_L$ and $P_M$ (BChls of the primary donor), $B_A$ and $B_B$ (monomeric BChls), $\Phi_A$ and $\Phi_B$ (BPhs), $Q_A$ (menaquinone) and $Q_B$ (ubiquinone) and the non-heme iron (Fe) and the location of Tyr M208 in wild type RCs from *B. viridis*. The hydrocarbon tails of the cofactors are omitted for clarity. The carotenoid and the tetraheme complex are also not shown. The 3-acetyl group of $\Phi_A$ is indicated by an arrow.

The mutation YF(M210) causes no significant alterations of the overall spatial structure of the *R. sphaeroides* RC [29]. Thus, the observed red shifts of ~3 nm of optical bands assigned to the monomeric BChl, $B_A$ [15,16,20,22], might be due to the removal of the OH dipole of Tyr M210. Furthermore, resonance Raman spectroscopy [30,31] as well as ENDOR spectroscopy of $P^{\bullet+}$ [25] and $\Phi_A^{\bullet-}$ [13] revealed that Tyr M210 is not engaged in hydrogen bonding to either cofactor. The same is true for Trp at position M210 as is evident from the X-ray structure of the respective mutant RC [32]. In contrast, a His at position M210 appears to form a hydrogen bond to the 3-acetyl group of $\Phi_A$ as judged from optical absorption spectra [15,22,31] and ENDOR spectroscopy of $\Phi_A^{\bullet-}$ [13].

An important result from ENDOR spectroscopy of $\Phi_A^{\bullet-}$ in *R. sphaeroides* is that the chemical nature and orientation of the amino acid side chain at position M210 influences the occurrence of the two subconformations $I_1^{\bullet-}$ and $I_2^{\bullet-}$. In particular, a Leu at position M210 suppresses the formation of the $I_2^{\bullet-}$ state, which has been explained by a steric hindrance of the 3-acetyl group that is exerted by the bulky side chain of Leu. This is the rationale for interpreting the two $\Phi_A^{\bullet-}$ states as torsional isomers of the 3-acetyl group (Fig. 2). Accordingly, the effect of His at position M210 on the electronic structure of $\Phi_A^{\bullet-}$ suggests that hydrogen bonding to the $3^1$-keto group forces the acetyl group to adopt an orientation that is distinct from those of the two states $I_1^{\bullet-}$ and $I_2^{\bullet-}$ [13].

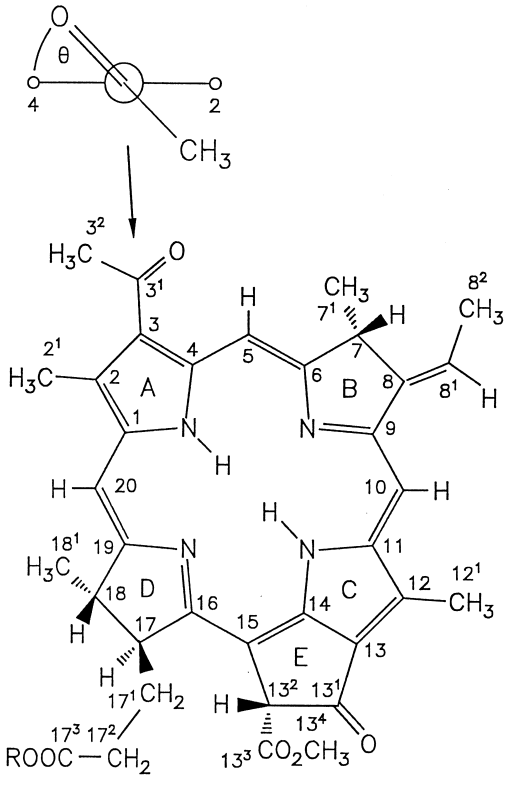


Fig. 2. Structure of BPh *b* with IUPAC numbering scheme (R = phytyl). The dihedral angle $\theta$ defining the orientation of the 3-acetyl group with respect to the macrocycle plane is given. The arrow indicates the viewing direction along the $C3^1$–C3 bond. In BPh *a* the $8$–$8^1$ bond is hydrogenated, i.e. the methyl group at position $8^2$ is not directly attached to the $\pi$ system.

In the case of *B. viridis* the tightly bound tetraheme complex facilitates the trapping of the radical anion $\Phi_A^{\bullet-}$ as compared with *R. sphaeroides* [9,10]. More important, electron tunneling between the *c*-type cytochromes and $P^{\bullet+}$ allows for trapping of the biradical $\Phi_A^{\bullet-}Q_A^{\bullet-}$ at low temperatures, since the double reduction of the $Q_A$ menaquinone is inhibited under these conditions [33–35]. Investigation of this biradical revealed that the changes of the optical absorption spectrum of RCs from *B. viridis* upon reduction of $\Phi_A$ are temperature-dependent [33]. In particular, it could be demonstrated that the absorbance difference spectrum due to the formation of the $\Phi_A^{\bullet-}Q_A^{\bullet-}$ biradical at 100 K undergoes irreversible changes upon raising the temperature to 200 K [34,35]. Shuvalov et al. proposed that these changes are due to an ET from $\Phi_A^{\bullet-}$ back to $B_A$ [34]. However, this possibility was ruled out by Tiede et al. who showed with EPR spectroscopy that the magnetic interaction of the two unpaired electrons in $\Phi_A^{\bullet-}Q_A^{\bullet-}$ is not significantly affected by the relaxation process, indicating that the electron of $\Phi_A^{\bullet-}$ does not move to $B_A$ [35]. Furthermore, these authors proposed on the basis of optical dichroism spectra that the relaxation affects the optical properties of the monomeric BChl $B_A$. They argued that structural relaxation of $B_A$ and/or its protein environment following the reduction of $\Phi_A$ at temperatures above 150 K is responsible for the observed effects.

In the present paper it is demonstrated that the structural relaxation processes following the formation of $\Phi_A^{\bullet-}Q_A^{\bullet-}$ [34,35] are correlated with the occurrence of the two subconformations $I_1^{\bullet-}$ and $I_2^{\bullet-}$ of $\Phi_A^{\bullet-}$ in RCs from *B. viridis*. Both ENDOR spectroscopy of $\Phi_A^{\bullet-}$ and optical spectroscopy of $\Phi_A^{\bullet-}Q_A^{\bullet-}$ are

applied to the wild type and the two site-directed mutants YF(M208) and YL(M208) [17]. The results suggest that torsional relaxation of the acetyl group of $\Phi_A$ most probably gives rise to the effects observed earlier by Shuvalov et al. [34] and Tiede et al. [35].

## 2. Materials and methods

### 2.1. Mutagenesis and protein isolation

The system for site-specific mutagenesis of *B. viridis* RCs has been described previously [36]. Mutations at position M208 were constructed and cells grown under phototrophic conditions as published earlier, and RCs were isolated by standard procedures [17]. The investigated wild type RCs were those of the $RC^-$ strain complemented with wild type genes (plasmid pRKML) [36]. For the investigation of the trapped radical anions the detergent LDAO was exchanged to Triton X-100 (Fluka, Biochemika) by dialysis.

### 2.2. EPR/ENDOR spectroscopy

EPR/ENDOR spectroscopy was performed on a Bruker ESP 300E spectrometer with home-built ENDOR accessories that are described in detail elsewhere [37,38]. Samples were prepared by mixing 90 μl of a solution containing 150–200 μM RC and 0.1% (w/v) Triton X-100 in 10 mM Tris–HCl (pH 8.0) with 10 μl of a freshly prepared 0.5 M $Na_2S_2O_4$ solution in 1 M Tris–HCl (pH 8.0) in an argon-flushed glass tube. Samples were illuminated in an ice-water bath for 2 min with white light using a 150 W halogen lamp before rapid freezing in liquid nitrogen. The illumination was continued during the freezing process, but not during the subsequent measurement [10].

### 2.3. Low temperature optical spectroscopy

Dark-adapted samples containing ~3 μM RC and 0.03% (w/v) Triton X-100 in 100 mM Tris–HCl (pH 8.0) and 65% (v/v) glycerol were thoroughly mixed with a hundredth volume of a freshly prepared 0.5 M $Na_2S_2O_4$ solution in 1 M Tris–HCl (pH 8.0) in a plastic cuvette of 1 cm path length and cooled to 100 K in a liquid nitrogen cryostat DN1704 (Oxford Instruments). The cryostat was mounted in the sample compartment of a Cary 05E spectrophotometer (Varian). All spectra were taken versus air in the reference compartment. The $\Phi_A^{\bullet-}Q_A^{\bullet-}$ state was generated by illumination of the samples in the cryostat at 100 K for 5–10 min with white light from a Schott KL1500 light source via an 8 mm light guide. The illumination was repeated until no further changes of the optical spectra could be induced, indicating complete trapping of the biradical. Relaxation of the trapped state was achieved by warming the sample in the cryostat to 200 K. Absorption spectra of the RCs in the relaxed state were measured after re-cooling to 100 K. Each temperature change took approximately 1 h.

## 3. Results

### 3.1. EPR/ENDOR spectroscopy of $\Phi_A^{\bullet-}$

The X-band EPR signal of $\Phi_A^{\bullet-}$ in RCs of *B. viridis*, trapped with 2 min illumination prior to freezing, shows no resolved hyperfine structure leading to an inhomogeneously broadened line centered at $g = 2.0036(2)$ with a peak-to-peak linewidth of $\Delta B_{pp} = 1.22 \pm 0.03$ mT. More detailed information about the hyperfine coupling (hfc) of certain nuclei can be obtained by ENDOR spectroscopy [10,11]. In the case of $^1$H-ENDOR each group of magnetically equivalent protons gives rise to two signals symmetrically spaced around the proton Larmor frequency $\nu_H$. The hfc constants $A$ can be calculated to first order from the observed resonance frequencies $\nu_{ENDOR}$ according to $A = 2|\nu_{ENDOR} - \nu_H|$. In microcrystalline samples (such as frozen solutions) the protons show characteristic ENDOR powder patterns [39]. In such spectra the resonances of methyl protons are most pronounced. For methyl groups that are directly attached to the π system (see Fig. 2) uniaxial hfc tensors with two components, $A_\perp$ and $A_\parallel$, are expected. The isotropic hfc constants are then given by $A_{iso} = (2A_\perp + A_\parallel)/3$ [11].

The spectrum of the wild type measured at 160 K (Fig. 3) exhibits the same hfcs as published for 100 K in an earlier report [10]. In contrast to BPh *a* there is

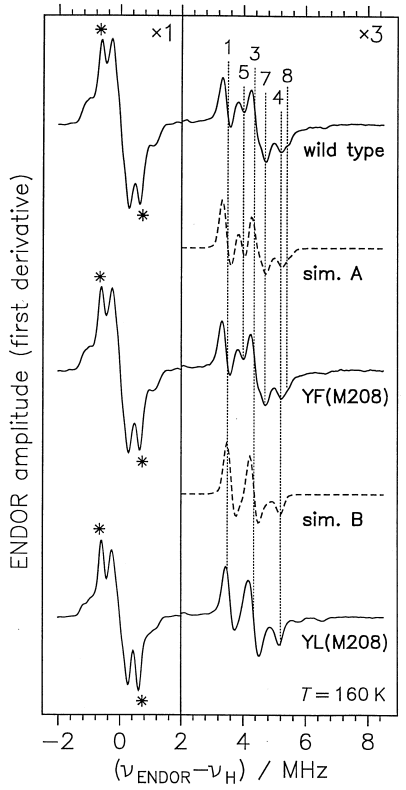


Fig. 3. High frequency part of the $^1$H-ENDOR spectra of freeze-trapped $\Phi_A^{\bullet-}$ in native and mutant RCs from *B. viridis* (solid spectra). The dashed spectra are simulations using four (sim. A) and two (sim. B) superimposed uniaxial hfc tensors; the tensor components are depicted in Table 1. The asterisks indicate a line pair assigned to the methyl protons at position $8^2$. Experimental conditions: microwave power 6.4 mW, rf power 200 W, rf modulation depth 140 kHz (frequency 12.5 kHz), time constant 164 ms (1024 data points, 60 scans).

an exocyclic double bond at ring B in BPh *b*, thus the methyl group at position $8^2$ is expected to also contribute strong signals to the spectra in addition to those at positions $2^1$ and $12^1$ (Fig. 2). However, on the basis of studies of BPh $b^{\bullet-}$ in organic solution [9–11], the hfc of these protons is expected to be small. Therefore, the intense line pair that occurs in the matrix ENDOR region (see asterisks in Fig. 3) and that is not observed in BPh $a^{\bullet-}$ [11] is tentatively assigned to the $A_\perp$ hfc component of the protons at position $8^2$. The magnitude of this component is of the order of $\sim$1 MHz and is only slightly decreased in YL(M208) as compared with the wild type and YF(M208).

In the range $(\nu_{ENDOR} - \nu_H) = 2$–8 MHz, six intense signals are resolved, which can be assigned to four uniaxial hfc tensors on the basis of spectral simulations (sim. A in Fig. 3; Table 1). Note that two of the eight tensor components are not resolved in the measured spectra. Since only two methyl groups (positions $2^1$ and $12^1$) in BPh $b^{\bullet-}$ give rise to large hfcs [9,10], the occurrence of four uniaxial hfc tensors indicates the presence of two distinct forms of $\Phi_A^{\bullet-}$. Essentially the same powder pattern was observed for $\Phi_A^{\bullet-}$ in *R. sphaeroides* under conditions where two states, termed $I_1^{\bullet-}$ and $I_2^{\bullet-}$, are present [12,13]. On the basis of the spectral analysis established for *R. sphaeroides* we assign the observed hfcs to tensor components of the protons at positions $2^1$ and $12^1$ (see Table 1).

The $^1$H-ENDOR spectrum of $\Phi_A^{\bullet-}$ in RCs of the mutant YF(M208) is identical to that of the wild type (Fig. 3). In the case of YL(M208) significant changes are observed in the range of the large methyl proton hfcs (Fig. 3, bottom). Only two uniaxial hfc tensors are observed, i.e. signals 5, 7 and 8 are absent (sim. B, Table 1). The same was found for the corresponding mutant YL(M210) of *R. sphaeroides* [13]. This indicates that in both species a Leu residue near the 3-acetyl group of $\Phi_A$ suppresses the formation of the $I_2^{\bullet-}$ state.

### 3.2. Low temperature optical spectroscopy of $\Phi_A^{\bullet-}Q_A^{\bullet-}$

The absorption spectra at 100 K of native and mutant RCs from *B. viridis* after chemical reduction of the quinones are shown in Fig. 4. The spectra are essentially similar, but the BChl $Q_x$ band shows a splitting in the mutants, whereas there is only one peak at 607 nm with a shoulder in the wild type. Furthermore, the two bands in the $Q_y$ region at $\sim$810 and 817 nm seen in the wild type and the Phe mutant are merged to one broad band at 815 nm in YL(M208).

The effects of trapping $\Phi_A^{\bullet-}$ in the presence of $Q_A^{\bullet-}$ by illumination at 100 K on the absorption spectrum can be seen from Fig. 5A,B for the case of the mutant YF(M208). The corresponding $\Phi_A^{\bullet-}/\Phi_A$ difference spectra for both mutants and the wild type are shown in Fig. 6 (dotted lines). In all cases, trapping of $\Phi_A^{\bullet-}$ results in selective bleaching of the $Q_x$ and $Q_y$ bands of $\Phi_A$ around 810 and 545 nm. These changes are accompanied by conservative electro-

Table 1
Hfc tensor components (MHz) of the $2^1$ and $12^1$ methyl protons obtained from spectral simulations of freeze-trapped $\Phi_A^{\bullet-}$ in native and mutant RCs of *B. viridis* as compared with the respective values of *R. sphaeroides*

| State | $I_1^{\bullet-}$ | | | | | | | $I_2^{\bullet-}$ | | | | | | |
|---|---|---|---|---|---|---|---|---|---|---|---|---|---|---|
| Molecular position[a] | $2^1$ | | | $12^1$ | | | | $2^1$ | | | $12^1$ | | | |
| Tensor components[b] | $A_\perp$ | $A_\parallel$ | $A_{iso}$ [c] | $A_\perp$ | $A_\parallel$ | $A_{iso}$ | $R$[d] | $A_\perp$ | $A_\parallel$ | $A_{iso}$ | $A_\perp$ | $A_\parallel$ | $A_{iso}$ | $R$ |
| Signal number | 1 | 2 | | 3 | 4 | | | 5 | 6 | | 7 | 8 | | |
| *B. viridis* | | | | | | | | | | | | | | |
| wild type | 6.8 | 8.3[f] | 7.3[f] | 8.6 | 10.5 | 9.2 | 1.26[g] | 7.8 | 9.4[f] | 8.3[f] | 9.1[f] | 11.0 | 9.7[f] | 1.17[h] |
| YF(M208) | 6.8 | 8.3[f] | 7.3[f] | 8.6 | 10.5 | 9.2 | 1.26[g] | 7.8 | 9.4[f] | 8.3[f] | 9.1[f] | 11.0 | 9.7[f] | 1.17[h] |
| YL(M208) | 7.1 | 8.6 | 7.6 | 8.6 | 10.4 | 9.2 | 1.21 | – | – | – | – | – | – | – |
| *R. sphaeroides*[e] | | | | | | | | | | | | | | |
| wild type | 6.6 | 8.1 | 7.1 | 8.5 | 10.4 | 9.1 | 1.28 | 7.7 | 9.4[f] | 8.3[f] | 9.1[f] | 11.0 | 9.7[f] | 1.17[h] |
| YF(M210) | 6.5 | 8.0 | 7.0 | 8.4 | 10.4 | 9.1 | 1.30 | 7.5 | 9.0[f] | 8.0[f] | 9.0[f] | 11.0 | 9.7[f] | 1.21[h] |
| YL(M210) | 6.8 | 7.9 | 7.2 | 8.3 | 10.2 | 8.9 | 1.24 | – | – | – | – | – | – | – |

[a]For numbering, see Fig. 2.
[b]Error of tensor components: ±100 kHz, if not indicated otherwise.
[c]$A_{iso} = (2A_\perp + A_\parallel)/3$; error: ±100 kHz, if not indicated otherwise.
[d]$R = A_{iso}(12^1)/A_{iso}(2^1)$; error: ±0.02, if not indicated otherwise.
[e]Data from [13].
[f]Error of these hfcs: ±200 kHz.
[g]Error: ±0.03.
[h]Error: ±0.04.

chromic shifts of the $Q_x$ band (red shift by ~1 nm) and the $Q_y$ band (blue shift by 6 nm) assigned to monomeric BChl *b* as well as a 3 nm blue shift of the long wavelength band of P at 999 nm. The formed radical anion of $\Phi_A$ itself causes new absorption bands at 683, 748 and 914 nm. The changes observed for wild type RCs are consistent with those reported in the literature [33–35]. Note that the *c*-type cytochromes absorb between 500 and 550 nm. Therefore, this spectral region is sensitive to changes of the redox state of the tetraheme complex.

Fig. 5C shows the absorption spectrum of YF(M208) after warming the illuminated sample in situ to 200 K and cooling back to 100 K, i.e. after structural relaxation of the state $\Phi_A^{\bullet-}Q_A^{\bullet-}$ in the dark. Fig. 6 (solid lines) represents the corresponding difference between the absorbance of the $\Phi_A^{\bullet-}Q_A^{\bullet-}$ state after relaxation and that of the initial state, $\Phi_A^0Q_A^{\bullet-}$, for both mutants and the wild type. A more detailed analysis of the absorption changes induced by the dark relaxation of the $\Phi_A^{\bullet-}Q_A^{\bullet-}$ state can be performed on the basis of double difference spectra (Fig. 7). These spectra are obtained by subtracting the dotted curve from the solid curve in Fig. 6. Hence, the positive bands in Fig. 7 correspond to the relaxed form and the negative bands to the unrelaxed form of $\Phi_A^{\bullet-}Q_A^{\bullet-}$. It is seen that there are distinct changes of bands that can be assigned to monomeric BChl as well as sharp absorption changes in the region of the cytochrome bands. The latter are probably due to temperature-dependent relaxation processes within the tetraheme complex.

In the case of the wild type (dashed line in Fig. 7, top) there is a pronounced absorption decrease at 825 nm in the $Q_y$ region of a BChl accompanied by the formation of two bands at 786 and 803 nm. In the $Q_x$ region a band is lost at 609 nm and another band formed at 642 nm. In addition, there is a small blue shift of a band around 680 nm corresponding to the absorption of the $\Phi_A$ radical anion. In order to assess the significance of these absorption changes we also investigated the changes that can be induced by warming a dark-adapted RC sample from 100 to 200 K and cooling back to 100 K (Fig. 7, bottom). Changes induced under these conditions are smaller by a factor of about 10 than the changes due to the dark relaxation of $\Phi_A^{\bullet-}Q_A^{\bullet-}$. The integral of the double difference spectrum between 575 and 900 nm is essentially zero, which indicates that the oscillator strength that is lost upon relaxa-

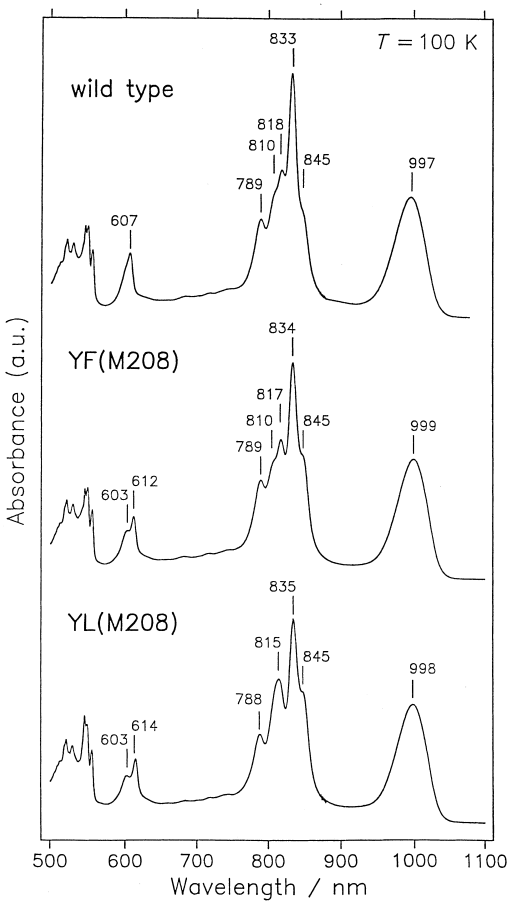


Fig. 4. Optical absorption spectra of dark-adapted RCs from *B. viridis* in the presence of 5 mM $Na_2S_2O_4$ in 100 mM Tris–HCl (pH 8.0), 65% (v/v) glycerol and 0.03% (w/v) Triton X-100 at $T = 100$ K. The bands at ~998 and ~845 nm are assigned to the lower and upper component, respectively, of the excitonically coupled BChl *b* dimer, P, on the basis of hole-burning studies [42]. The bands at 603 and 607 nm in the wild type are assigned to the $Q_x$ transitions of $B_B$ and $B_A$, respectively, but only the latter is red-shifted in the mutants; for the assignment of the bands at 818 and 833 nm, see Fig. 5. The bands at 789 and 810 nm are due the $Q_y$ transitions of $\Phi_B$ and $\Phi_A$, respectively; the $\Phi_A$ band is red-shifted in YL(M208). Experimental parameters (Setup Cary 05E, Varian): spectral bandwidth, 1 nm; detector change, 860–880 nm; averaging time, 0.0667 s; data interval, 0.1 nm.

tion of $\Phi_A^{\bullet-}Q_A^{\bullet-}$ is recovered in the newly formed bands.

The absorption changes due to the structural relaxation of $\Phi_A^{\bullet-}Q_A^{\bullet-}$ in YF(M208) are similar to those of the wild type, but shifts of both the negative and positive bands are observed (Fig. 7, top). The amplitude of the 786 nm band is significantly reduced in the mutant, probably in favor of the 809 nm band, and is close to the error limits for this spectral range. In the case of the mutant YL(M208) warming RCs in the state $\Phi_A^{\bullet-}Q_A^{\bullet-}$ to 200 K and cooling back to 100 K causes only slight changes of the $\Phi_A^{\bullet-}/\Phi_A$ difference spectrum (Figs. 6 and 7). This clearly indicates that the structural relaxation of $\Phi_A^{\bullet-}Q_A^{\bullet-}$ as observed

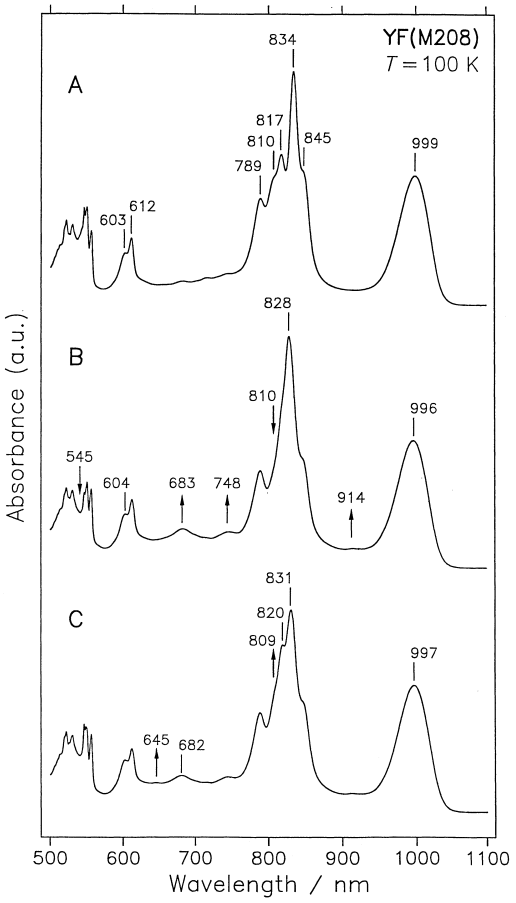


Fig. 5. Optical absorption spectra of RCs from the *B. viridis* mutant YF(M208) at $T = 100$ K taken sequentially on the same sample. (A) Dark-adapted sample after chemical reduction of the quinones (same as in Fig. 4). (B) $\Phi_A^{\bullet-}Q_A^{\bullet-}$ state as formed after illumination with white light at $T = 100$ K; the arrows indicate the bands that are bleached (↓) or formed (↑) upon illumination. Note the selective bleaching of the 810 nm band assigned to $\Phi_A$. The band at 834 nm (in A) assigned to $B_A$ is blue-shifted because of an electrochromic effect due to reduction of $\Phi_A$. The band at 817 nm assigned to $B_B$ remains unaffected, but is superimposed on the shifted band of $B_A$ at 828 nm. The assignment of the bands to either $B_A$ or $B_B$ is tentative, since mixing between the $Q_y$ transitions cannot be excluded [40,41]. (C) $\Phi_A^{\bullet-}Q_A^{\bullet-}$ state at $T = 100$ K after relaxation at $T = 200$ K in the dark; the arrows indicate the newly formed bands.

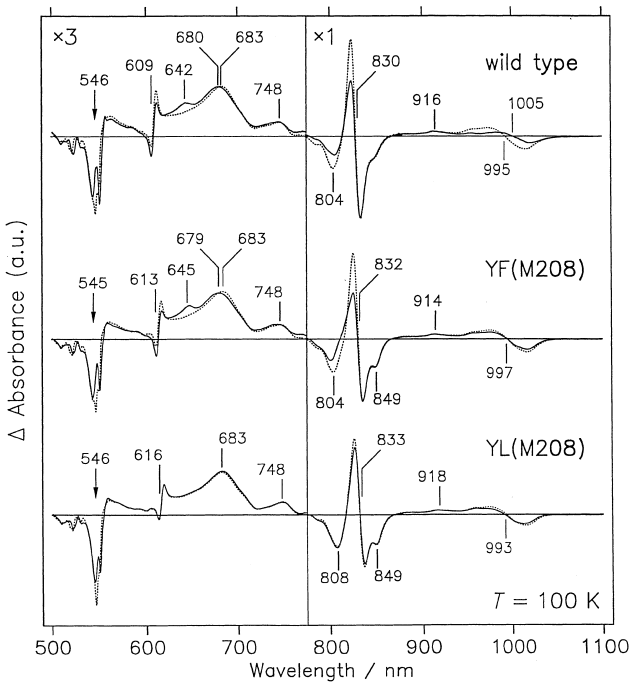


Fig. 6. Optical $\Phi_A^{\bullet-}Q_A^{\bullet-}/\Phi_A^0Q_A^{\bullet-}$ difference spectra at $T=100$ K of native and mutant RCs from *B. viridis* before (dotted lines) and after (solid lines) relaxation at 200 K in the dark (see text). The spectra are normalized to the maximal absorbance change around 914 nm. The arrows indicate the bleaching of the $Q_x$ band of $\Phi_A$ that is superimposed on changes of cytochrome bands.

in the wild type and the mutant YF(M208) does *not* take place in the mutant YL(M208). In the corresponding double difference spectrum the only changes that are larger than the experimental uncertainties correspond to shifts of cytochrome bands between 500 and 550 nm and a red shift of the 830 nm band (Fig. 7, center). The latter suggests that a temperature-dependent relaxation of a BChl might take place, which is, however, qualitatively and quantitatively distinct from the changes observed in the wild type and the Phe mutant.

## 4. Discussion

### 4.1. Two distinct conformations of $\Phi_A^{\bullet-}$

We have shown that the freeze-trapped BPh *b* radical anion in photosynthetic RCs from *B. viridis* is actually a mixture of two distinct conformations of $\Phi_A^{\bullet-}$. A similar result has recently been found for the BPh *a* radical anion in *R. sphaeroides*. However, in the case of *R. sphaeroides* we were able to obtain spectra with different proportions of the two states under appropriate experimental conditions, i.e. by variation of the temperature and the illumination time prior to freezing [12,13]. This made it possible to create difference spectra that directly correspond to the two states $I_1^{\bullet-}$ and $I_2^{\bullet-}$. In the case of *B. viridis* the ENDOR spectra are insensitive to such a variation of experimental conditions. This indicates that the processes occurring during the trapping of $\Phi_A^{\bullet-}$ prior to freezing are somewhat different in the two species.

In the case of *R. sphaeroides* the two states $I_1^{\bullet-}$ and $I_2^{\bullet-}$ were interpreted as different torsional isomers of the 3-acetyl group of $\Phi_A$ on the basis of semi-empirical molecular orbital calculations and studies of site-directed mutants [12,13]. Since both the spatial structure of the RC and the electronic structure of $\Phi_A^{\bullet-}$

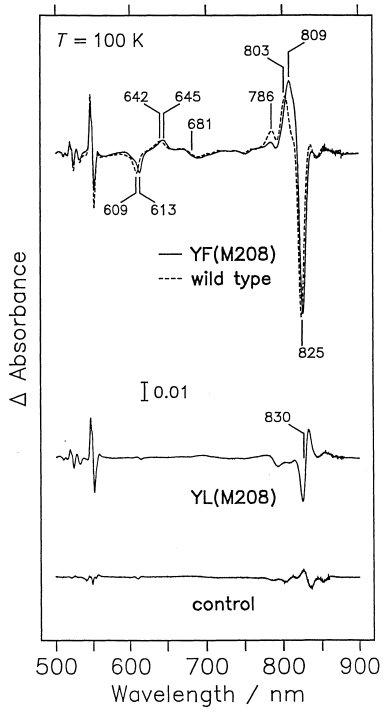


Fig. 7. Double difference spectra obtained by subtracting the two corresponding spectra shown in Fig. 6. The positive peaks belong to the relaxed form and the negative peaks to the unrelaxed form of $\Phi_A^{\bullet-}Q_A^{\bullet-}$; for assignment of bands, see Section 4.3. The control corresponds to the absorbance difference induced in a dark-adapted sample of YF(M208) by warming to $T=200$ K and re-cooling to $T=100$ K without illumination.

are similar in *B. viridis* as compared with *R. sphaeroides*, we interpret the data of the former as resulting from the same effect. One can estimate from the spectral simulations that most RCs from *B. viridis* are in the $I_1^{\bullet-}$ conformation after relaxation of $\Phi_A^{\bullet-}$, whereas in *R. sphaeroides* $I_2^{\bullet-}$ predominates. This suggests that the energy surface for the torsional motion of the acetyl group is somewhat different in the two cases. The reason for this difference is not clear at present. In both cases, however, the side chain of Leu distorts this energy surface in such a way that the $I_2^{\bullet-}$ state is no longer populated and the acetyl group is forced to adopt an orientation similar to the $I_1^{\bullet-}$ state in the wild type. The latter point is important, since it demonstrates that in the Leu mutant only one of the two conformational substates of the photoactive BPh exists. This information is used in the following to interpret the optical absorption spectra.

### 4.2. Irreversible change of $\Phi_A^{\bullet-}Q_A^{\bullet-}$

The optical spectra show that the biradical state $\Phi_A^{\bullet-}Q_A^{\bullet-}$ exists in at least two forms in the wild type and the mutant YF(M208) of *B. viridis*. The low temperature state formed at 100 K is characterized by a prominent bleaching of bands assigned to $\Phi_A$ and electrochromic shifts of bands assigned to monomeric BChls. In addition, the state exhibits bands that are characteristic for a BPh *b* radical anion [9]. In the relaxed form an absorbance increase is superimposed on the bleaching of the $Q_y$ band of the neutral $\Phi_A$. The corresponding $Q_x$ band remains essentially unaffected as do the absorption bands assigned to $\Phi_A^{\bullet-}$, indicating that the changes in the $Q_y$ region are not due to an ET from $\Phi_A^{\bullet-}$ back to $B_A$ in accordance with the results of Tiede et al. [35]. The absence of these changes in the mutant YL(M208) indicates that the ability of the biradical to undergo this particular structural relaxation is correlated with the presence of the $I_2^{\bullet-}$ subconformation of the $\Phi_A^{\bullet-}$ radical anion. On the basis of our interpretation of the two subconformations as torsional isomers of the 3-acetyl group of $\Phi_A$ [12,13] we therefore assign the optical changes observed in the wild type and the Phe mutant to a reorientation of this acetyl group, i.e. to a change of the angle $\theta$ (see Fig. 2).

To further elucidate the relationship between the observed optical changes and the electronic structure of $\Phi_A$ it would be desirable to perform ENDOR spectroscopy on the biradical state $\Phi_A^{\bullet-}Q_A^{\bullet-}$. This is, however, more complicated, since hfcs of nuclei from both $\Phi_A^{\bullet-}$ and $Q_A^{\bullet-}$ are expected to contribute to the spectra. A direct trapping of $\Phi_A^{\bullet-}$ at low temperatures would be possible with quinone-depleted RCs, but $Q_A$ removal has not yet been accomplished with *B. viridis* RCs. Work along these lines is in progress.

### 4.3. Interpretation of optical spectra

It is well known from studies on various bacterial RCs that local perturbations induced by site-directed mutations have specific effects on the optical properties of nearby cofactors. For instance, mutations at position M208 near $B_A$ in *R. capsulatus* RCs cause a splitting of the BChl $Q_x$ band indicating a shift of the low energy transition that contributes to this band [15]. On the other hand, mutations at the symmetry-related position L181 near $B_B$ shift the high energy shoulder of the BChl $Q_x$ band [15]. This is interpreted in such a way that there are two distinct transitions in the $Q_x$ region, which are to first order located on $B_A$ and $B_B$, respectively. Similar effects on the corresponding $Q_x$ region are observed for mutations in the vicinity of either of the two BPhs [12]. This suggests that at least for the $Q_x$ transitions an assignment of certain bands to distinct cofactors is possible. In *B. viridis* the YF(M208) mutation also causes a splitting of the BChl $Q_x$ band corresponding to a shift of only the low energy transition from 607 to 612 nm. The same mutation causes a red shift of both the negative and the positive band in the $Q_x$ region in the double difference spectrum (Fig. 7, top). Therefore, we assign these bands to transitions that are mainly located on $B_A$. The situation is more complicated for the $Q_y$ region, where a significant mixing between transitions of the six bacteriochlorins is expected [40,41]. This impedes an assignment of distinct bands to individual cofactors. However, the strong effect of the YF(M208) mutation on the $Q_y$ bands in the double difference spectra (Fig. 7, top) suggests that transitions of $B_A$ are somehow involved in these bands. In summary, we conclude that the acetyl reorientation mainly influences the optical properties of $B_A$. This conclusion is in agreement with the assignment of Tiede et al. [35].

Time-resolved optical spectroscopy is important for understanding the early events in photosynthetic charge separation. The detailed interpretation of the difference spectra is, however, difficult and is usually performed by assigning a certain time-independent spectrum to each of the intermediate states. It is clear that this approach is too simple and misleading if a state undergoes a structural relaxation during its lifetime. An obvious conclusion from our data is that torsional relaxation of the 3-acetyl group of $\Phi_A$ could contribute to the transient optical difference spectra. The M208 mutations open a way to further investigate this problem.

## 5. Conclusions

We found evidence that the 3-acetyl group of the photoactive bacteriopheophytin, $\Phi_A$, in RCs of *B. viridis* can adopt different distinct orientations as was also found in RCs of *R. sphaeroides* [12,13]. The effect of acetyl reorientation on the electronic structure of $\Phi_A^{\bullet-}$ is quite similar in the two bacterial species. A bulky amino acid residue (e.g. Leu) in the vicinity of the acetyl group (at position M208 in *B. viridis*) is able to lock this group in one distinct orientation. This effect can be used to interpret irreversible changes observed in optical $\Phi_A^{\bullet-}/\Phi_A$ difference spectra between 100 and 200 K [34,35]. The torsional relaxation of the 3-acetyl group of $\Phi_A$ appears to particularly affect the optical absorption properties of the monomeric BChl, $B_A$, which is the primary electron acceptor [3,25]. These results might, therefore, be of importance for the interpretation of transient optical spectra and for the understanding of the primary steps of light-induced charge separation in bacterial RCs.

## Acknowledgements

We thank I. Geisenheimer and R. Kunert (both TU Berlin) for technical assistance. The software used to simulate ENDOR powder patterns was written by Dr. H. Käss at the TU Berlin. This work was supported by DFG (Sfb 312, TP A4/A5) and Fonds der Chemischen Industrie to W.L.

## References

[1] J. Deisenhofer, O. Epp, I. Sinning, H. Michel, J. Mol. Biol. 246 (1995) 429–457.
[2] C.R.D. Lancaster, U. Ermler, H. Michel, in: R.E. Blankenship, M.T. Madigan, C.E. Bauer (Eds.), Anoxygenic Photosynthetic Bacteria, Kluwer, Dordrecht, 1995, pp. 503–526.
[3] W. Zinth, W. Kaiser, in: J. Deisenhofer, J.R. Norris (Eds.), The Photosynthetic Reaction Center, Vol. II, Academic Press, San Diego, CA, 1993, pp. 71–88.
[4] A.R. Holzwarth, M.G. Müller, Biochemistry 35 (1996) 11820–11831.
[5] I.H.M. van Stokkum, L.M.P. Beekman, M.R. Jones, M.E. van Brederode, R. van Grondelle, Biochemistry 36 (1997) 11360–11368.
[6] J.M. Peloquin, J.C. Williams, X. Lin, R.G. Alden, A.K.W. Taguchi, J.P. Allen, N.W. Woodbury, Biochemistry 33 (1994) 8089–8100.
[7] G. Hartwich, H. Lossau, M.E. Michel-Beyerle, A. Ogrodnik, J. Phys. Chem. B 102 (1998) 3815–3820.
[8] M.Y. Okamura, R.A. Isaacson, G. Feher, Biochim. Biophys. Acta 546 (1979) 394–417.
[9] M.S. Davis, A. Forman, L.K. Hanson, J. Fajer, J. Phys. Chem. 83 (1979) 3325–3332.
[10] W. Lubitz, B. Bönigk, M. Plato, R.A. Isaacson, M.Y. Okamura, G. Feher, in: M. Baltscheffsky (Ed.), Current Research in Photosynthesis, Vol. I, Kluwer, Dordrecht, 1990, pp. 141–144.
[11] W. Lubitz, in: H. Scheer (Ed.), Chlorophylls, CRC Press, Boca Raton, FL, 1991, pp. 903–944.
[12] F. Müh, J.C. Williams, J.P. Allen, W. Lubitz, Biochemistry 37 (1998) 13066–13074.
[13] F. Müh, M.R. Jones, W. Lubitz, Biospectroscopy 5 (1999) 35–46.
[14] A. Hiraishi, Int. J. Syst. Bacteriol. 47 (1997) 217–219.
[15] T.J. DiMagno, P.D. Laible, N.R. Reddy, G.J. Small, J.R. Norris, M. Schiffer, D.K. Hanson, Spectrochim. Acta A 54 (1998) 1247–1267.
[16] K.A. Gray, J.W. Farchaus, J. Wachtveitl, J. Breton, D. Oesterhelt, EMBO J. 9 (1990) 2061–2070.
[17] M. Bibikova, T. Arlt, W. Zinth, D Oesterhelt, in: P. Mathis (Ed.), Photosynthesis: from Light to Biosphere, Vol. I, Kluwer, Dordrecht, 1995, pp. 867–870.
[18] U. Finkele, C. Lauterwasser, W. Zinth, K.A. Gray, D. Oesterhelt, Biochemistry 29 (1990) 8517–8521.
[19] C.-K. Chan, L.X.-Q. Chen, T.J. DiMagno, D.K. Hanson, S.L. Nance, M. Schiffer, J.R. Norris, G.R. Fleming, Chem. Phys. Lett. 176 (1991) 366–372.
[20] V. Nagarajan, W.W. Parson, D. Davis, C.C. Schenck, Biochemistry 32 (1993) 12324–12336.
[21] W. Zinth, T. Arlt, J. Wachtveitl, Ber. Bunsen-Ges. Phys. Chem. 100 (1996) 1962–1966.
[22] L.M.P. Beekman, I.H.M. van Stokkum, R. Monshouwer, A.J. Rijnders, P. McGlynn, R.W. Visschers, M.R. Jones, R. van Grondelle, J. Phys. Chem. 100 (1996) 7256–7268.

[23] W.W. Parson, V. Nagarajan, D. Gaul, C.C. Schenck, Z.-T. Chu, A. Warshel, in: M.E. Michel-Beyerle (Ed.), Reaction Centers of Photosynthetic Bacteria, Springer, Berlin, 1990, pp. 239–249.
[24] R.G. Alden, W.W. Parson, Z.-T. Chu, A. Warshel, J. Phys. Chem. 100 (1996) 16761–16770.
[25] J. Wachtveitl, H. Huber, R. Feick, J. Rautter, F. Müh, W. Lubitz, Spectrochim. Acta A 54 (1998) 1231–1245.
[26] M.E. van Brederode, M.R. Jones, R. van Grondelle, Chem. Phys. Lett. 268 (1997) 143–149.
[27] M.E. van Brederode, M.R. Jones, F. van Mourik, I.H.M. van Stokkum, R. van Grondelle, Biochemistry 36 (1997) 6855–6861.
[28] M.E. van Brederode, J.P. Ridge, I.H.M. van Stokkum, F. van Mourik, M.R. Jones, R. van Grondelle, Photosynth. Res. 55 (1998) 141–146.
[29] A.J. Chirino, E.J. Lous, M. Huber, J.P. Allen, C.C. Schenck, M.L. Paddock, G. Feher, D.C. Rees, Biochemistry 33 (1994) 4584–4593.
[30] T.A. Mattioli, K.A. Gray, M. Lutz, D. Oesterhelt, B. Robert, Biochemistry 30 (1991) 1715–1722.
[31] M.R. Jones, M. Heer-Dawson, T.A. Mattioli, C.N. Hunter, B. Robert, FEBS Lett. 339 (1994) 18–24.
[32] P.K. Fyfe, K.E. McAuley-Hecht, J.P. Ridge, S.M. Prince, G. Fritzsch, N.W. Isaacs, R.J. Cogdell, M.R. Jones, Photosynth. Res. 55 (1998) 133–140.
[33] A. Verméglio, G. Paillotin, Biochim. Biophys. Acta 681 (1982) 32–40.
[34] V.A. Shuvalov, A.Ya. Shkuropatov, M.A. Ismailov, in: J. Biggins (Ed.), Progress in Photosynthesis Research, Vol. I, Martinus Nijhoff, The Hague, 1987, pp. 161–168.
[35] D.M. Tiede, E. Kellogg, J. Breton, Biochim. Biophys. Acta 892 (1987) 294–302.
[36] E. Laußermair, D. Oesterhelt, EMBO J. 11 (1992) 777–783.
[37] J. Rautter, F. Lendzian, W. Lubitz, S. Wang, J.P. Allen, Biochemistry 33 (1994) 12077–12084.
[38] W. Zweygart, R. Thanner, W. Lubitz, J. Magn. Reson. Ser. A 109 (1994) 172–176.
[39] J.S. Hyde, G.H. Rist, L.E.G. Eriksson, J. Phys. Chem. 72 (1968) 4269–4275.
[40] W.W. Parson, A. Warshel, J. Am. Chem. Soc. 109 (1987) 6152–6163.
[41] M.A. Thompson, M.C. Zerner, J. Am. Chem. Soc. 113 (1991) 8210–8215.
[42] N.R.S. Reddy, S.V. Kolaczkowski, G.J. Small, Science 260 (1993) 68–71.